

*Citation for published version:*

Aljalamdeh, R, Price, R, Jones, M & Bolhuis, A 2021, 'The effect of particle size of inhaled tobramycin dry powder on the eradication of *Pseudomonas aeruginosa* biofilms', *European Journal of Pharmaceutical Sciences*, vol. 158, 105680. <https://doi.org/10.1016/j.ejps.2020.105680>

*DOI:*

[10.1016/j.ejps.2020.105680](https://doi.org/10.1016/j.ejps.2020.105680)

*Publication date:*

2021

*Document Version*

Peer reviewed version

[Link to publication](#)

**University of Bath**

**Alternative formats**

If you require this document in an alternative format, please contact:  
[openaccess@bath.ac.uk](mailto:openaccess@bath.ac.uk)

**General rights**

Copyright and moral rights for the publications made accessible in the public portal are retained by the authors and/or other copyright owners and it is a condition of accessing publications that users recognise and abide by the legal requirements associated with these rights.

**Take down policy**

If you believe that this document breaches copyright please contact us providing details, and we will remove access to the work immediately and investigate your claim.

1 **The effect of particle size of inhaled tobramycin dry powder on the eradication of**  
2 ***Pseudomonas aeruginosa* biofilms**

3

4 Reham Aljalamdeh, Robert Price, Matthew D. Jones, and Albert Bolhuis\*

5

6 Department of Pharmacy and Pharmacology, University of Bath, Bath BA2 7AY, United  
7 Kingdom

8

9 \*Corresponding author: email: [a.bolhuis@bath.ac.uk](mailto:a.bolhuis@bath.ac.uk), phone +44 (0)1225 383813

10 **Abstract**

11 *Pseudomonas aeruginosa* is the predominant opportunistic bacterium that causes chronic  
12 respiratory infections in cystic fibrosis (CF) patients. This bacterium can form biofilms, which  
13 are structured communities of cells encased within a self-produced matrix. Such biofilms have  
14 a high level of resistance to multiple classes of antibiotics. A widely used treatment of *P.*  
15 *aeruginosa* lung infections in CF patients is tobramycin dry powder inhalation. The behaviour  
16 of particles in the lung has been well studied, and dry powder inhalers are optimised for optimal  
17 dispersion of the drug into different zones of the lung. However, one question that has not been  
18 addressed is whether the size of an antibiotic particle influences the antibiofilm activity against  
19 *P. aeruginosa*. We investigated this by fractionating tobramycin particles using a Next  
20 Generation Impactor (NGI). The fractions obtained were then tested in an *in vitro* model on  
21 *P. aeruginosa* biofilms. The results indicate that the antibiofilm activity of tobramycin dry  
22 powder inhaler can indeed be influenced by the particle size. Against *P. aeruginosa* biofilms  
23 of two clinical isolates, smaller tobramycin particles (aerodynamic diameter <2.82 µm) showed  
24 better efficacy by approximately 20% as compared to larger tobramycin particles (aerodynamic  
25 diameter <11.7 µm) However, this effect was only observed when biofilms were treated for 3  
26 hours, whereas there was no difference after treatment for 24 hours. This suggests that in our  
27 model the rate of dissolution of larger particles limits the effectiveness of tobramycin over a 3-  
28 hour time period, which is relevant as this is equivalent to the time in which most tobramycin  
29 is cleared from the lung.

30

31 **Keywords:** *Pseudomonas aeruginosa*, biofilms, tobramycin, dry powder inhaler, Next  
32 Generation Impactor (NGI), particle size

## 33 1. Introduction

34 In patients with cystic fibrosis (CF), the opportunistic pathogen *Pseudomonas aeruginosa* is a  
35 major cause of lung infections leading to increased morbidity and mortality rates among these  
36 patients. This is attributed partially to the ability of this bacterium to form biofilms (Ciofu et  
37 al., 2015; Muheim et al., 2017; Nikaido and Pagès, 2012). These biofilms are highly organized  
38 communities of cells that are attached to each other and/or to surfaces, and embedded within a  
39 self-synthesized extracellular polymeric substance (EPS) matrix, mainly containing  
40 extracellular DNA, polysaccharides, and/or proteins (Furiga et al., 2015). Biofilms are  
41 characterized by a high tolerance to both immune defensive mechanisms and to most of the  
42 available antibiotic therapies. For instance, it is assumed that cells inside biofilms are 10-1000  
43 times less susceptible to anti-microbial therapies as compared to planktonic free-floating cells  
44 (Marshall et al., 2016; Patton et al., 2010; She et al., 2018).

45 *P. aeruginosa* biofilms in CF lungs settle and localise in a thick mucus layer in the trachea-  
46 bronchial region of the respiratory airways (Geller et al., 2011). Such a location makes the  
47 treatment of these infections using the systemic delivery of antibiotic agents challenging, as  
48 high doses are required to reach the lung tissue which can lead to adverse reactions. Therefore,  
49 the pulmonary delivery of antibiotics is an attractive approach for the treatment of lung CF  
50 infections (Geller et al., 2011; Worlitzsch et al., 2002). Inhaled antibacterial drugs that are  
51 used in the treatment of *P. aeruginosa* CF lung infections are in two forms, being either  
52 nebulized solutions or dry powder formulations (Ambrus et al., 2018). The currently approved  
53 inhaled dry powder antibiotics are colistin and tobramycin. For instance, TOBI Podhaler® is  
54 an approved dry powder inhalation formulation of tobramycin (McKeage, 2013; Akkerman-  
55 Nijland et al, 2020), which most CF patients prefer when comparing to nebulised tobramycin,  
56 leading to, for instance, better adherence (Harrison et al., 2014). Tobramycin powder from a  
57 capsule is aerosolized using the Podhaler device by the energy of the patient's own inspiration

58 (Konstan et al., 2011), resulting in the particles in the powder being separated from each other  
59 and carried in the airstream to the lungs where they deposited.

60 Following inhalation, these particles distribute and deposit into different compartments of the  
61 lung. Briefly, the lung can be divided into two regions, the conducting and the respiratory  
62 zones. The conducting zone includes trachea, bronchi, bronchioles, and terminal bronchioles,  
63 whereas the respiratory zone comprises of the respiratory bronchioles, alveolar ducts and  
64 alveolar sacs (Hoiby, 2011). Deposition of dry powder particles in these zones depends on  
65 several variables such as patient-associated factors, the inhaler device and inhaled powder  
66 formulation properties (Tiddens et al., 2014) such as particle shape, density and size.

67 Drug particle size is one of the important properties that can influence both the deposition and  
68 fate of particles in the respiratory airways. Normally, inhaled drug particles are polydisperse  
69 in nature with a large particle size range (Deng et al., 2018). Particles with an aerodynamic  
70 diameter ( $d_{ae}$ ) larger than 10  $\mu\text{m}$  are mostly deposited in the oropharyngeal region and do not  
71 reach the lungs, and those that are between 3-10  $\mu\text{m}$  are mostly deposited in the trachea-  
72 bronchial region. Furthermore, particles at a range of 1-3  $\mu\text{m}$  target the alveolar zone of the  
73 lungs (Geller et al., 2011; Nafee et al., 2014; Verbanck et al., 2006), but those that even smaller  
74 ( $<1 \mu\text{m}$ ) are exhaled due to low inertial and gravitational forces which are insufficient to  
75 deposit them (Nafee et al., 2014). Once deposited, the particles must dissolve and the rate of  
76 this depends on the size of these particles, which in turn can influence drug efficacy (Nafee et  
77 al., 2014).

78 Currently, studies that evaluate the *in vitro* activity of tobramycin rely on testing its efficacy  
79 against *P. aeruginosa* biofilms in an aqueous solution. However, there are no biofilm models  
80 to test dry powder formulations, and it is thus unclear what the effect of, for instance, particle  
81 size is on antibiofilm activity, highlighting the need for a model that can address such issues.  
82 To achieve this, we used a Next Generation Impactor (NGI), which is an instrument used to

83 measure *in vitro* behaviour of inhalable dry powder products (Rowland et al., 2018). The NGI  
84 sequentially separates drug aerosols into various size categories from larger to smaller particles  
85 on the basis of the particles' aerodynamic diameter (Guo et al., 2008; Roberts and Mitchell,  
86 2013; Wang et al., 2017). The cut-off aerodynamic diameters of these particles were previously  
87 determined at flow rates of 30 and 60 L/min (Marple et al., 2003). Using the NGI and a recently  
88 developed aerosol dose collection apparatus, we fractionated tobramycin particles into  
89 different sizes and tested these on a *P. aeruginosa* biofilm models to (a), test the feasibility of  
90 analysing dry powders on biofilms and (b), to further understand the role of particle size on  
91 antibiotic efficacy, which could be very valuable for improving the pharmacological activity  
92 of inhaled antibiotics.

93 **2. Materials and Methods**

94 **2.1 Chemicals**

95 All chemicals and culture media were purchased from Sigma-Aldrich (Gillingham, UK) or  
96 Fisher Scientific (Loughborough, UK), unless stated otherwise. The TOBI Podhaler® and 28  
97 mg tobramycin inhalation powder (TIP) capsules were purchased from Novartis  
98 Pharmaceuticals (Camberley, UK). Tobramycin that was used to determine the minimal  
99 inhibitory concentration (section 2.3) and a calibration curve (section 2.8) was purchased from  
100 Fisher Scientific (97% purity).

101

102 **2.2 Bacterial strains and growth media**

103 The bacterial strains used in this study are laboratory strain *P. aeruginosa* PAO1 (Stover et al.,  
104 2000) and three clinical CF isolates LMG 27648, LMG 27643, and LMG 27649. These clinical  
105 *P. aeruginosa* isolates were obtained from the Belgian Coordinated Collections of  
106 Microorganisms (BCCM, Brussels, Belgium). Strains were routinely grown on Mueller Hinton  
107 (MH; Oxoid) broth. Artificial sputum media (ASM) and minimal MOPS medium (MMM)  
108 were prepared as described elsewhere (Kirchner et al., 2012; LaBauve and Wargo, 2012).

109

110 **2.3 Minimum inhibitory concentration (MIC)**

111 MIC tests were performed in MH, MMM and ASM using the macro-dilution protocol as  
112 described elsewhere (Andrews, 2001). The MIC is defined as the lowest concentration of an  
113 antibiotic agent that shows no visible growth of a microorganism after overnight incubation.

114

115 **2.4 Colony biofilm assay**

116 Colony biofilms of *P. aeruginosa* were grown as described (Merritt et al., 2005). Briefly, sterile  
117 semipermeable polycarbonate membranes (Whatman, Little Chalfont, UK; 0.2  $\mu\text{m}$  pore size,  
118 25 mm) were placed on the surface of MH agar plates. Then an aliquot of 50  $\mu\text{l}$  of overnight  
119 culture, adjusted to an optical density (OD) at 600 nm of 0.05, was spotted on each membrane.  
120 After that, the inoculated membranes were incubated for 48 h at 37°C to permit biofilm  
121 formation. The polycarbonate membranes were moved to fresh agar plates with sterile forceps  
122 on a daily basis. On the third day, a 30  $\mu\text{g}$  tobramycin disc (Oxoid), or a glass fibre filter with  
123 TIP of various sizes (see section 2.6) were placed on the biofilms using sterile forceps. In case  
124 of the glass fibre filter, TIP particles were in direct contact with the top of the biofilms, and  
125 controls were covered with a filter without tobramycin. A schematic of the colony biofilm with  
126 tobramycin filter is shown in Figure 1. The biofilms were then incubated for a further 3 h or  
127 24 h, after which cells were harvested by resuspension in 5 mL of sterile phosphate buffered  
128 saline (PBS). Cells were dispersed by vigorously vortexing, and the colony forming units were  
129 determined by serial dilution and plating.

130

## 131 **2.5 Tobramycin capsule filling and humidity control**

132 To collect similar amounts of TIP with different particle sizes, we adjusted the mass of TIP  
133 aerosolised into the NGI. Before each experiment, hydroxypropyl methylcellulose capsules  
134 (HPMC; transparent; size #3; Capsugel, Colmar, France) were filled manually with TIP  
135 extracted from TOBI Podhaler® capsules and weighed using a four-place analytical balance  
136 (Sartorius, Epsom, UK). Initial experiments found unacceptable variation in NGI deposition  
137 when capsules were filled immediately before use. Therefore, capsules were stored for 24 h in  
138 a sealed desiccator under a controlled temperature of 25°C and relative humidity (RH) of 43%  
139 before testing, resulting in acceptable reproducibility. This RH was produced using a saturated



140 salt solution of potassium carbonate ( $K_2CO_3$ ) (Miller et al., 2017). Temperature and relative  
141 humidity were monitored using a thermohygrometer placed inside the desiccator, and the  
142 following day these capsules were aerosolised through the NGI as described below (section  
143 2.6).

144

## 145 **2.6 Operation of the NGI**

146 The NGI was used by applying conditions described elsewhere (Meenach et al., 2013). Briefly,  
147 before testing, the pre-separator was filled with 15mL Milli-Q water. The NGI stages were  
148 coated with a solution of 1% (v/v) glycerol in methanol (VWR Chemicals) to minimize particle  
149 bounce. The NGI was connected to twin vacuum pumps (GAST 1023 series, connected in  
150 parallel) via a critical flow controller (TPK, Copley, Nottingham, UK), which was fixed before  
151 each experiment at 30 L/min or 60 L/min flow rates using a digital flow meter (DFM2000,  
152 Copley Scientific, Nottingham, UK). A TIP capsule for each experiment was aerosolised from  
153 a Podhaler through the NGI for 10 seconds, which was chosen as it is sufficient for complete  
154 dispersion of the powder from the capsule.

155 Initial experiments were carried out to determine the aerodynamic particle size distribution of  
156 TIP when aerosolised from the Podhaler at 30 L/min and 60 L/min. These experiments utilised  
157 all eight stages of the NGI and the aerosolization of 28 mg TIP from a single as supplied TOBI  
158 capsule (n=5). Following each aerosolization, the mass of tobramycin collected on the  
159 induction port, pre-separator, stages 1 to 7, and MOC was determined (section 2.8).

160 Subsequently, TIP particles of different sizes were collected from either stage 2 or 4 using an  
161 Aerosol Dose Collection (ADC) device (Price et al., 2020). The ADC allows particles to be  
162 collected on a glass fibre filter without the formation of *in situ* agglomerates, which can affect  
163 their subsequent dissolution behaviour. In the experimental set up with the ADC, a rubber

164 stopper was placed in the NGI air outlet from stage 2 or stage 4 to disrupt airflow and ensure  
165 the collection of all TIP particles on the filter. Second, a glass fibre filter (Copley®, 25 mm  
166 diameter, 1 µm pore size) was mounted in the ADC to collect TIP particles. The glass fibre  
167 filter was replaced for each repeat of the experiment and the flow rate was adjusted for each  
168 experiment after placing the filter in the ADC. These filters were either applied directly to  
169 biofilms (section 2.4), particles were visualised by electron microscopy (section 2.7), or the  
170 mass of TIP collected was determined (section 2.8).

171

## 172 **2.7 Scanning Electron Microscopy (SEM)**

173 To demonstrate that the ADC apparatus had successfully captured TIP particles of different  
174 sizes, their geometric particle size distribution was determined using SEM. TIP particles on  
175 glass fibre filters were analysed by applying conditions stated elsewhere (Li et al., 2014). TIP  
176 samples were fixed into aluminium stubs (Agar Scientific, Stansted, UK) using double-sided  
177 adhesive carbon tabs (Agar Scientific). Then, the samples were coated with a thin film of gold  
178 using a sputter coater (Sputter Coater S 150B, Edwards, Burgess Hill, UK). The coating process  
179 was operated at 1 kV of voltage for 3 min. The images were captured using Jeol SEM (Jeol  
180 Jsm-6480LV Scanning Electron Microscope; Jeol Ltd, Welwyn Garden City, UK), and several  
181 magnifications levels were used. The captured images were further analysed for geometric  
182 particle size determination using the software package ImageJ (Schneider et al., 2012). For  
183 every ImageJ analysis, manual particle size measurements were performed, and for every  
184 measurement fixed criteria were used: all particles in the given image might be measured, even  
185 the small particles in front of large particles; a specific number (100) of particles were selected  
186 randomly and the same magnification (x5000) was used for all images. As TOBI Podhaler®  
187 particles are spherical (McKeage, 2013), particle size was not sensitive to the direction of

188 measurement, so all diameters were measured in the vertical direction. Particle size  
189 distributions were summarised by the median diameter and span, which was defined the  
190 difference between the ninetieth and tenth centile diameters, divided by the median diameter.

191

## 192 **2.8 High Performance Liquid Chromatography-Mass Spectrometry (HPLC-MS)** 193 **quantification**

194 To determine the mass of tobramycin collected on parts of the NGI or glass fibre filters, they  
195 were rinsed with known volumes of Milli-Q water and sonicated for 10 min in an ultrasonic  
196 water bath to ensure complete dissolution of TIP. To quantify the amount of tobramycin, an  
197 HPLC-MS method was developed and validated. The chromatographic system consisted of a  
198 pentafluoro phenyl F5 column (2.6  $\mu$ M, 2.1 x 100 mm; Phenomenex, Macclesfield, UK) as the  
199 stationary phase, which was used with a flow rate of 0.3 mL/min at 25°C and an injection  
200 volume of 10  $\mu$ L of each sample was injected in triplicate. The mobile phase involved utilizing  
201 two solvents, which were 100% water with 0.1% (v/v) formic acid as solvent A and 100%  
202 methanol with 0.1% (v/v) formic acid as solvent B. The proportion of these solvents in the  
203 mobile phase was controlled during the analysis by the ultra HPLC instrument. Elution was  
204 carried out with 0% mobile phase B for 3 min followed by a linear gradient to 100% B for 7  
205 min. The mass spectrometer (Bruker Daltonik GmbH, Bremen, Germany) was operated in  
206 electrospray time of flight (ESI) positive-ion MS mode, and the following conditions were used  
207 during the MS analysis. The capillary voltage was set to 4500 V, nebulizing gas at 4 bar, and  
208 drying gas at 12 L/min at 220°C. The concentration of tobramycin in injected samples (and  
209 thus the mass of deposited tobramycin) was determined by constructing a calibration curve  
210 using kanamycin as an internal standard. Following the addition of kanamycin (final  
211 concentration 4  $\mu$ g/mL), samples were vigorously vortexed prior to HPLC-MS analysis. All

212 stock solutions were prepared on the same day of the experiment, and HPLC-MS analysis was  
213 performed with 24 h. The calibration curve was linear ( $r^2= 0.998$ ) over the range of 5 to 20  
214  $\mu\text{g/ml}$ . Based on the standard deviation of y-intercepts of the regression line (International  
215 Conference on Harmonisation, 1996), the estimates for the limit of detection was 1.4  $\mu\text{g/ml}$   
216 and the limit of quantification was 4.4  $\mu\text{g/ml}$ .

217

## 218 **2.10 Statistical analysis**

219 Data were presented as the mean  $\pm$  standard error of the mean (SEM) of  $n \geq 3$  independent  
220 biological repeats. Results were analysed using GraphPad Prism 7 by applying the Student *t*-  
221 test. Values of  $p < 0.05$  were considered statistically significant.

222

## 223 3. Results

### 224 3.1 The *in vitro* activity of tobramycin against *P. aeruginosa*

225 The MICs (Table 1) of tobramycin against one laboratory strain (*P. aeruginosa* PAO1) and  
226 three clinical CF isolates (*P. aeruginosa* LMG 27648, LMG 27643, and LMG 27649) were  
227 determined in MH broth, MMM and ASM by the macro-dilution method. The results showed  
228 that MIC values in in MH broth and MMM were fairly similar and differed by at most one  
229 doubling dilution, in the range of 0.25-1 µg/mL The MIC was, for all four strains, 4 µg/mL  
230 when ASM was used. All strains were susceptible to tobramycin according to BSAC  
231 breakpoints.

232 To determine the activity of tobramycin against *P. aeruginosa* biofilms, which is the state that  
233 the cells are in during a lung infection, a colony biofilm assay was used. This model was chosen  
234 as the biofilm grow on a semi-solid surface with an air interface, which is probably more  
235 representative of biofilms in the lung as compared to the more standard 96-well plate assay in  
236 which biofilms are completely immersed in liquid. The results showed that in all tested strains,  
237 tobramycin reduced the viable count in the biofilms moderately (Fig 2). However, complete  
238 eradication was not achieved and the reduction in viable count was, on average, approximately  
239 60%.

240

### 241 3.2 Aerodynamic particle size distribution of tobramycin inhalation powder

242 The aerodynamic particle size distributions of TIP aerosolised from the Podhaler at both 30  
243 L/min and 60 L/min are shown in Fig 3.

244

### 245 3.3 Tobramycin masses collected with the ADC mounted on stages 2 or 4 of the NGI

246 To determine the effect of particle size on eradication of *P. aeruginosa* biofilms, it was  
247 necessary to collect the same amount of TIP but with different particle sizes. The parameters  
248 to obtain approximately 0.5 mg TIP per filter were determined in an empirical manner. To this  
249 purpose we used the ADC mounted onto the NGI and determined that, at stage 2 at 30 L/min  
250 and TIP capsule mass of 4.4 mg, we collected a very similar mass as when using stage 4 at 60  
251 L/min and TIP capsule mass of 4.3 mg. This resulted in a mean mass of 0.51 mg with SD value  
252 of 0.05 for larger particles (stage 2 at 30 L/min,  $d_{ac} < 11.7 \mu\text{m}$ ) and 0.48 mg with SD value of  
253 0.12 for smaller particles (stage 4 at 60 L/min,  $d_{ac} < 2.82 \mu\text{m}$ ), with a difference between those  
254 masses of 7.8%. Statistically, the difference between the masses was not significant ( $p=0.15$ ).

255

### 256 **3.4 SEM analysis**

257 Before testing fractionated tobramycin particles on biofilms, a number of tests were performed.  
258 Firstly, SEM analysis was used to image TIP particles that had been extracted from the NGI  
259 stages using the method outlined in section 2.6. These SEM images were further analysed to  
260 obtain geometric particle size measurements using ImageJ software. Representative SEM  
261 micrographs for TIP particles (Fig 4) show polydisperse, approximately spherical, and porous  
262 microparticles. The geometric particle size distributions determined from these images, using  
263 ImageJ, were approximately log-normal (Fig 5) and showed that on stage 2 at 30 L/min, the  
264 particle size distribution included some coarse particles, with a median geometric diameter of  
265  $5.6 \mu\text{m}$  and span of 1.5. The particles collected at stage 4 at 60 L/min had a smaller median  
266 geometric diameter of  $1.4 \mu\text{m}$  and span of 1.2.

267

268

269 **3.5 The influence of differently sized tobramycin inhalation powder particles against *P.***  
270 ***aeruginosa* biofilms**

271 The fractions of small and large TIP particles were used to challenge *P. aeruginosa* biofilms.  
272 These were treated with a dose of 0.5 mg/filter TIP, and filters without tobramycin were used  
273 as control. The biofilms were incubated for 3 h, as this period is comparable to the time it takes  
274 for tobramycin sputum concentrations to be significantly reduced in people with CF (Hubert et  
275 al., 2009; Poli et al., 2007). The 3 h treatment time was not particularly effective in killing cells  
276 in our biofilm model but, crucially, there was an approximate 20% reduction of the viable count  
277 when applying particles with  $d_{ac} < 2.82 \mu\text{m}$  as compared with particles with  $d_{ac} < 11.7 \mu\text{m}$  (Fig  
278 6). For *P. aeruginosa* LMG27649 and LMG27643, particles with  $d_{ac} < 11.7 \mu\text{m}$  did not have  
279 any effect on the biofilms, but there was a statistically significant (LMG27649:  $p=0.04$ ;  
280 LMG27643:  $p=0.02$ ) reduction with particles with  $d_{ac} < 2.82 \mu\text{m}$ . For the other two strains,  
281 larger particles had a moderate effect on the viable count of cells in biofilms and there was a  
282 further reduction in viable count when the biofilms were treated with smaller particles.  
283 However, in the latter cases this reduction was statistically not significant (LMG27648:  
284  $p=0.26$ ; PAO1:  $p=0.63$ ).

285 The reduction in viable count after a 3 h treatment of the biofilms was rather poor, so we also  
286 tested the effect of a 24 h incubation with TIP. In this case, the reduction in viable count was  
287 between 80-90% when comparing samples with the untreated control (Fig 7). However, there  
288 was no significant difference in viable count reduction when comparing small and large TIP  
289 particles.

290

#### 291 4. Discussion

292 We investigated the influence of differently sized TIP particles against *P. aeruginosa* biofilms  
293 by making use of the NGI to separate particles into different fractions. These particles were  
294 collected from stage 2 at 30 L/min and stage 4 at 60 L/min, meaning that the collected fractions  
295 had  $d_{ac} < 11.7 \mu\text{m}$  and  $d_{ac} < 2.82 \mu\text{m}$ , respectively (Marple et al., 2003). The efficiency of the  
296 NGI and ADC device at capturing particles of different size ranges was confirmed by the SEM  
297 analysis, which found particles captured at stage 2 at 30 L/min had a larger median geometric  
298 diameter ( $5.6 \mu\text{m}$ ) than those captured at stage 4 at 60 L/min ( $1.4 \mu\text{m}$ ).

299 An aerosol collection apparatus was used to collect TIP particles from the above-mentioned  
300 stages. Without this, deposition of particles from the NGI occurs directly on a solid impactor  
301 stage with high-speed deposition of particles in a small area, which results in the formation of  
302 strong agglomerates which then behave as larger particles (Price et al., 2020). However, using  
303 the ADC apparatus enables a slow and uniform deposition of aerosol particles over a single,  
304 large surface area glass fibre filter, so the collected powder subsequently behaves as single  
305 particles.

306 A difficult issue to resolve was that the NGI separates powder into size fractions with different  
307 masses for each fraction, while equal masses were required to analyse the effect of particle size  
308 only. Moreover, the amount of tobramycin collected did not vary in a linear fashion with the  
309 aerosolised dose, so was difficult to predict. We essentially had to use a trial and error process  
310 to determine the parameters to collect equal masses of differently sized particles. Another issue  
311 was that initially the mass of TIP collected from the ADC device was variable, but results  
312 became more consistent when capsules were equilibrated at a constant humidity and  
313 temperature, before use.



314 When antibiotic particles are deposited on a biofilm, they must first dissolve in order to exert  
315 their pharmacological activity. This depends on particle size, which is one of the parameters  
316 that determines physical properties of a drug (Shekunov et al., 2007; Wang et al., 2017).  
317 Accordingly, the influence of TIP particles was investigated by testing differently sized  
318 particles for 3 and 24 h. At 24 h, there was a significant reduction in the viable count when  
319 comparing treated with untreated samples, but there was no difference between smaller and  
320 larger particles. Thus, over 24 h the difference in the rate of dissolution of small and large TIP  
321 particles is not a rate limiting step. However, this time is not physiologically relevant, as  
322 tobramycin sputum concentrations are significantly reduced after just 3 h in people with CF  
323 (Hubert et al., 2009; Poli et al., 2007), with the TOBI Podhaler having a sputum half-life of  
324 only 1-2 hours (Geller et al., 2007). An incubation time of 3 h was thus more appropriate. This  
325 time period was far less effective in reducing the viable count but, importantly, smaller particles  
326 were more effective by approximately 20% when compared to larger particles. Indeed, it is  
327 generally recognized that the dissolution rate of small-sized particles can be significantly better  
328 than the larger-sized particles, which is attributed to the larger specific surface area of the small  
329 particles (Riley et al., 2012; Tay et al., 2018; van der Wiel et al., 2017; Watts and Williams,  
330 2011). We should note, however, that while we observed a difference in the effectivity between  
331 small and large particles for all *P. aeruginosa* strains, it was statistically significant only for  
332 the two clinical isolates that were the most recalcitrant to a 3 h treatment, (LMG27649 and  
333 LMG27643). In these strains, larger particles did not cause any reduction in the viable count,  
334 while small particles resulted in a 20% reduction. In case of the other strains (LMG27648 and  
335 PAO1), larger particles resulted in approximately 15-20% reduction in viable count, with a  
336 further non-significant reduction with smaller particles. Planktonic cells of those four strains  
337 all displayed the same sensitivity to tobramycin, but phenotypic and genetic differences  
338 between the strains could result in the differences in biofilm formation, such as in composition

339 of the extracellular matrix or thickness of the biofilms (Wimpenny et al., 2000). For example,  
340 the three clinical isolates are reported to be alginate producers (Hoffmann et al., 2005; Leitão  
341 et al., 1996; Mathee et al., 2008), whereas the laboratory strain PAO1 does not produce this  
342 polysaccharide. We also observed that only LMG 27649 was unable to grow in a minimal  
343 growth medium without the addition of casamino acids (data not shown), indicating that this  
344 strain is auxotrophic, whereas the other strains are not. Whether this would influence the effects  
345 of tobramycin particles is not known, but it does clearly show that the strains differ from each  
346 other.

347 The influence of differently sized particles of other drugs has been evaluated previously,  
348 showing better efficacy for smaller sized particles as compared to larger (Jinno et al., 2006;  
349 Leach et al., 2009; Liu et al., 2015). For example, for the oral vasodilator cilostazol, smaller  
350 cilostazol particles of 2.4  $\mu\text{m}$  had a better rate of dissolution and efficacy than particles of 13  
351  $\mu\text{m}$  (Jinno et al., 2006). This was also observed for inhaled beclomethasone (a corticosteroid),  
352 which is more effective in a particle size of 1.1  $\mu\text{m}$  as compared to 4  $\mu\text{m}$  (Leach et al., 2009;  
353 Van Schayck and Donnell, 2004; Vanden Burgt et al., 2000). Although these differences have  
354 been attributed to varying lung deposition patterns with changing particle size, they may also  
355 have been influenced the faster dissolution rate of smaller particles.

356 We should acknowledge that our study has limitations. Firstly, there was a slight difference in  
357 the TIP mass that were collected for small and large sized particles from different stages/flow  
358 rates. It was technically difficult to obtain equal masses of differently sized particles, in  
359 particular at the amounts required for biofilm assays (0.5 mg/filter). However, the difference  
360 in the amounts obtained was statistically not significant ( $p > 0.05$ ). It should be noted that on  
361 average we collected slightly less (<8%) of the smaller particles, but these were nevertheless  
362 more effective, which only strengthens our conclusion that smaller particle sizes result in more  
363 efficient killing of cells in *P. aeruginosa* biofilms.

364 Another limitation is that with the NGI the maximum particle size that is collected on the filters  
365 can be controlled, but not the minimum particle size. Thus, while the average particle size  
366 differs between the collected fractions, there is some overlap in particle sizes and effects on  
367 antibiofilm activity could have been greater if it was technically possible to control both  
368 minimum and maximum sizes. Also, our SEM analysis only measured the diameters of a small  
369 number of particles (100). Despite this, we obtained log-normal particle size distributions (Fig  
370 5), so these data provide additional reassurance that the NGI and ADC device collected  
371 particles of different sizes.

372 Our system used the *in vitro* colony biofilm model (Merritt et al., 2005). It is a simple model  
373 system but nevertheless it is useful as biofilm grows on a semi-solid surface with an air-  
374 interface. It is of course not the same as the conditions found in a lung, but in this study, it was  
375 a more useful model than for instance the standard 96-well plate biofilm assay. It should also  
376 be noted that 0.5 mg/filter TIP as used here is actually a very large dose when compared to a  
377 therapeutic dose of 112 mg spread through the whole surface area of the lungs (Geller et al.,  
378 2011). Future studies therefore need to focus on the use of models that, firstly, use an amount  
379 of antibiotic that better reflects clinical doses and, secondly, better mimic the *in vivo* lung  
380 pathological conditions. The latter could be achieved using, for instance, *ex vivo* models that  
381 use porcine lung samples (Harrison and Diggle, 2016), or *in vivo* models (Kukavica-Ibrulj and  
382 Levesque, 2008).

383 Our hypothesis on the effect of particle size was only tested for one dry powder inhaled  
384 antibiotic, tobramycin. An important aim of our study was to establish a system to test dry  
385 powder inhalers on biofilms. This has now been achieved and has demonstrated that the particle  
386 size of inhaled dry powders can influence their anti-biofilm activity. These are the most  
387 significant aspects of these findings, as this tool can be used to test other antibiotics. Our system  
388 may be of particular relevance to the development of dry powder inhaled formulations of drugs

389 with a low aqueous solubility, as in this situation the differences between small and large  
390 particles may become more pronounced than for tobramycin (which is freely soluble in water).  
391 Investigation of this issue may therefore highlight additional ways to increase the effectiveness  
392 of poorly soluble inhaled drugs. Future research should also measure the dissolution rate of  
393 different antibiotic particle size fractions, to fully examine the potential relationship between  
394 anti-biofilm activity and particle dissolution.

## 395 **5. Conclusion**

396 Tobramycin dry powder inhaler is one of the most widely used inhaled antibiotics in the  
397 treatment of CF lung infections. Here we showed that small TIP particles ( $d_{ac} < 2.82 \mu\text{m}$ )  
398 showed better efficacy as indicated by a 20% reduction in the viable count as compared to  
399 larger particles ( $d_{ac} < 11.7 \mu\text{m}$ ) at an incubation time of 3 h against *P. aeruginosa* biofilms; this  
400 reduction was statistically significant for two strains of the four strain, but the trend was  
401 observed in all strains. This short incubation time is important, as this is the same timeframe in  
402 which tobramycin is largely cleared from the lung. These initial findings highlight that particle  
403 size can affect TIP antibiofilm activity. Importantly, we have developed a system to test the  
404 effect of dry powder inhalers on bacterial biofilms, and we are planning to utilise this to test  
405 other antibiotics and as well as employing more advanced biofilm models.

406

## 407 **Acknowledgements**

408 We thank Shaun Reeksting and Christian Rehbein for their help with HPLC analysis, and we  
409 are grateful to the Philadelphia University (Jordan) for a fully funded scholarship to RA.

410 **References**

- 411 Akkerman-Nijland, A.M., Yousofi, M., Rottier, B.L, van der Vaart, H., Burgerhof, J.G.M.,  
412 Frijlink, H.W., Touw D.J., Koppelman G.H., Akkerman, O.W., 2020. Eradication of  
413 *Pseudomonas aeruginosa* in cystic fibrosis patients with inhalation of dry powder  
414 tobramycin. *Ther Adv Respir Dis.* 14, 1753466620905279
- 415 Ambrus, R., Benke, E., Farkas, A., Balashazy, I., Szabo-Revesz, P., 2018. Novel dry powder  
416 inhaler formulation containing antibiotic using combined technology to improve aerodynamic  
417 properties. *Eur. J. Pharm. Sci.* 123, 20-27.
- 418 Andrews, J.M., 2001. Determination of minimum inhibitory concentrations. *J. Antimicrob.*  
419 *Chemother.* 48 Suppl 1, 5-16.
- 420 Buttini, F., Brambilla, G., Copelli, D., Sisti, V., Balducci, A.G., Bettini, R., Pasquali, I., 2016.  
421 Effect of flow rate on in vitro aerodynamic performance of NEXThaler® in comparison with  
422 Diskus® and Turbohaler® dry powder inhalers. *J. Aerosol Med. Pulm. Drug Deliv.* 29, 167-  
423 178.
- 424 Ciofu, O., Tolker-Nielsen, T., Jensen, P.O., Wang, H., Hoiby, N., 2015. Antimicrobial  
425 resistance, respiratory tract infections and role of biofilms in lung infections in cystic fibrosis  
426 patients. *Adv. Drug. Deliv. Rev.* 85, 7-23.
- 427 Deng, Q., Ou, C., Chen, J., Xiang, Y., 2018. Particle deposition in tracheobronchial airways of  
428 an infant, child and adult. *Sci. Total Environ.* 612, 339-346.
- 429 Furiga, A., Lajoie, B., El Hage, S., Baziard, G., Roques, C., 2015. Impairment of *Pseudomonas*  
430 *aeruginosa* biofilm resistance to antibiotics by combining the drugs with a new quorum-  
431 sensing inhibitor. *Antimicrob. Agents Chemother.* 60, 1676-1686.
- 432 Geller, D.E., Konstan, M.W., Smith, J., Noonberg, S., Conrad, C., 2007. Novel Tobramycin  
433 Inhalation Powder in Cystic Fibrosis Subjects: Pharmacokinetics and Safety. *Pediatr Pulmonol*  
434 42, 307-313.

435 Geller, D.E., Weers, J., Heurding, S., 2011. Development of an inhaled dry-powder  
436 formulation of tobramycin using PulmoSphere technology. *J. Aerosol Med. Pulm. Drug Deliv.*  
437 24, 175-182.

438 Guo, C., Gillespie, S.R., Kauffman, J., Doub, W.H., 2008. Comparison of delivery  
439 characteristics from a combination metered-dose inhaler using the Andersen cascade impactor  
440 and the next generation pharmaceutical impactor. *J. Pharm. Sci.* 97, 3321-3334.

441 Harrison, F., Diggle, S.P., 2016. An ex vivo lung model to study bronchioles infected with  
442 *Pseudomonas aeruginosa* biofilms. *Microbiology* 162, 1755-1760.

443 Harrison, M.J., McCarthy, M., Fleming, C., Hickey, C., Shortt, C., Eustace, J.A., Murphy,  
444 D.M., Plant, B.J. 2014. Inhaled versus nebulised tobramycin: a real world comparison in adult  
445 cystic fibrosis (CF). *J. Cyst. Fibros.* 13, 692-698.

446 Hoffmann, N., Rasmussen, T.B., Jensen, P.O., Stub, C., Hentzer, M., Molin, S., Ciofu, O.,  
447 Givskov, M., Johansen, H.K., Hoiby, N., 2005. Novel mouse model of chronic *Pseudomonas*  
448 *aeruginosa* lung infection mimicking cystic fibrosis. *Infect. Immun.* 73, 2504-2514.

449 Hoiby, N., 2011. Recent advances in the treatment of *Pseudomonas aeruginosa* infections in  
450 cystic fibrosis, *BMC Med.*, 9, 32.

451 Hubert, D., Leroy, S., Nove-Josserand, R., Murriss-Espin, M., Mely, L., Dominique, S., Delaisi,  
452 B., Kho, P., Kovarik, J.M., 2009. Pharmacokinetics and safety of tobramycin administered by  
453 the PARI eFlow® rapid nebulizer in cystic fibrosis. *J Cyst Fibros* 8, 332-337.

454 International Conference on Harmonization (ICH) of Technical Requirements for the  
455 Registration of Pharmaceuticals for Human Use, 1996. Validation of analytical procedures:  
456 Text and Methodology. ICH-Q2B, Geneva.

457 Jinno, J.-i., Kamada, N., Miyake, M., Yamada, K., Mukai, T., Odomi, M., Toguchi, H.,  
458 Liversidge, G.G., Higaki, K., Kimura, T., 2006. Effect of particle size reduction on dissolution

459 and oral absorption of a poorly water-soluble drug, cilostazol, in beagle dogs. *J. Control.*  
460 *Release* 111, 56-64.

461 Kirchner, S., Fothergill, J.L., Wright, E.A., James, C.E., Mowat, E., Winstanley, C., 2012. Use  
462 of artificial sputum medium to test antibiotic efficacy against *Pseudomonas aeruginosa* in  
463 conditions more relevant to the cystic fibrosis lung, *J. Vis. Exp.*, e3857-e3857.

464 Konstan, M.W., Flume, P.A., Kappler, M., Chiron, R., Higgins, M., Brockhaus, F., Zhang, J.,  
465 Angyalosi, G., He, E., Geller, D.E., 2011. Safety, efficacy and convenience of tobramycin  
466 inhalation powder in cystic fibrosis patients: The EAGER trial. *J. Cyst. Fibros.* 10, 54-61.

467 Kukavica-Ibrulj, I., Levesque, R.C., 2008. Animal models of chronic lung infection with  
468 *Pseudomonas aeruginosa*: useful tools for cystic fibrosis studies. *Lab. Anim.* 42, 389-412.

469 LaBauve, A.E., Wargo, M.J., 2012. Growth and laboratory maintenance of *Pseudomonas*  
470 *aeruginosa*. *Curr. Protoc. Microbiol.* 25, 6E.1.1-6E.1.8.

471 Leach, C., Colice, G.L., Luskin, A., 2009. Particle size of inhaled corticosteroids: Does it  
472 matter? *J. Allergy Clin. Immunol.* 124, S88-S93.

473 Leitão, J.H., Alvim, T., Sá-Correia, I., 1996. Ribotyping of *Pseudomonas aeruginosa* isolates  
474 from patients and water springs and genome fingerprinting of variants concerning mucoidy.  
475 *FEMS Immunol. Med. Microbiol.* 13, 287-292.

476 Li, X., Vogt, F.G., Hayes, D., Jr., Mansour, H.M., 2014. Design, characterization, and aerosol  
477 dispersion performance modeling of advanced co-spray dried antibiotics with mannitol as  
478 respirable microparticles/nanoparticles for targeted pulmonary delivery as dry powder inhalers.  
479 *J. Pharm. Sci.* 103, 2937-2949.

480 Liu, D., Pan, H., He, F., Wang, X., Li, J., Yang, X., Pan, W., 2015. Effect of particle size on  
481 oral absorption of carvedilol nanosuspensions: in vitro and in vivo evaluation. *Int. J.*  
482 *Nanomedicine* 10, 6425-6434.

483 Marple, V., Roberts, D., Romay, F., C Miller, N., G Truman, K., Van Oort, M., Olsson, B., J  
484 Holroyd, M., Mitchell, J., Hochrainer, D., 2003. Next Generation Pharmaceutical Impactor (A  
485 New Impactor for Pharmaceutical Inhaler Testing). Part I: Design. J. Aerosol Med. Pulm. Drug  
486 Deliv. 16, 283-299.

487 Marshall, L.J., Oguejiofor, W., Price, R., Shur, J., 2016. Investigation of the enhanced  
488 antimicrobial activity of combination dry powder inhaler formulations of lactoferrin. Int. J.  
489 Pharm. 514, 399-406.

490 Mathee, K., Narasimhan, G., Valdes, C., Qiu, X., Matewish, J.M., Koehrsen, M., Rokas, A.,  
491 Yandava, C.N., Engels, R., Zeng, E., Olavarietta, R., Doud, M., Smith, R.S., Montgomery, P.,  
492 White, J.R., Godfrey, P.A., Kodira, C., Birren, B., Galagan, J.E., Lory, S., 2008. Dynamics of  
493 *Pseudomonas aeruginosa* genome evolution. Proc. Natl. Acad. Sci. U. S. A. 105, 3100-3105.

494 McKeage, K., 2013. Tobramycin inhalation powder: a review of its use in the treatment of  
495 chronic *Pseudomonas aeruginosa* infection in patients with cystic fibrosis. Drugs 73, 1815-  
496 1827.

497 Meenach, S.A., Vogt, F.G., Anderson, K.W., Hilt, J.Z., McGarry, R.C., Mansour, H.M., 2013.  
498 Design, physicochemical characterization, and optimization of organic solution advanced  
499 spray-dried inhalable dipalmitoylphosphatidylcholine (DPPC) and  
500 dipalmitoylphosphatidylethanolamine poly(ethylene glycol) (DPPE-PEG) microparticles and  
501 nanoparticles for targeted respiratory nanomedicine delivery as dry powder inhalation aerosols.  
502 Int J Nanomedicine 8, 275-293.

503 Merritt, J.H., Kadouri, D.E., O'Toole, G.A., 2005. Growing and analyzing static biofilms, Curr.  
504 Protoc. Microbiol., Ch 1, Unit-1B.1.

505 Miller, D.P., Tan, T., Nakamura, J., Malcolmson, R.J., Tarara, T.E., Weers, J.G., 2017.  
506 Physical characterization of tobramycin inhalation powder: II. State diagram of an amorphous  
507 engineered particle formulation. Mol. Pharm. 14, 1950-1960.



508 Muheim, C., Gotzke, H., Eriksson, A.U., Lindberg, S., Lauritsen, I., Norholm, M.H.H., Daley,  
509 D.O., 2017. Increasing the permeability of *Escherichia coli* using MAC13243, *Sci. Rep.* 7,  
510 17629.

511 Nafee, N., Husari, A., Maurer, C.K., Lu, C., de Rossi, C., Steinbach, A., Hartmann, R.W., Lehr,  
512 C.M., Schneider, M., 2014. Antibiotic-free nanotherapeutics: ultra-small, mucus-penetrating  
513 solid lipid nanoparticles enhance the pulmonary delivery and anti-virulence efficacy of novel  
514 quorum sensing inhibitors. *J. Control. Release* 192, 131-140.

515 Nikaido, H., Pagès, J.-M., 2012. Broad-specificity efflux pumps and their role in multidrug  
516 resistance of Gram-negative bacteria. *FEMS Microbiol. Rev.* 36, 340-363.

517 Patton, J.S., Brain, J.D., Davies, L.A., Fiegel, J., Gumbleton, M., Kim, K.J., Sakagami, M.,  
518 Vanbever, R., Ehrhardt, C., 2010. The particle has landed - characterizing the fate of inhaled  
519 pharmaceuticals. *J. Aerosol Med. Pulm. Drug Deliv.* 23 Suppl 2, S71-87.

520 Poli, G., Acerbi, D., Pennini, R., Raschini, A.S., Carrado, M.E., Eichler, H.G., Eichler, I., 2007.  
521 Clinical Pharmacology Study of Bramitob®, a Tobramycin Solution for Nebulization, in  
522 Comparison with Tobi®. *Pediatr. Drugs.* 9 Suppl 1, 3-9.

523 Price, R., Shur, J., Ganley, W., Farias, G., Fotaki, N., Conti, D.S., Delvadia, R., Absar, M.,  
524 Saluja, B., Lee, S., 2020. Development of an Aerosol dose Collection Apparatus for in vitro  
525 dissolution measurements of orally inhaled drug products. *AAPS J* 22, 47.

526 Riley, T., Christopher, D., Arp, J., Casazza, A., Colombani, A., Cooper, A., Dey, M., Maas, J.,  
527 Mitchell, J., Reiners, M., Sigari, N., Tougas, T., Lyapustina, S., 2012. Challenges with  
528 developing in vitro dissolution tests for orally inhaled products (OIPs). *AAPS PharmSciTech*  
529 13, 978-989.

530 Roberts, D.L., Mitchell, J.P., 2013. The effect of nonideal cascade impactor stage collection  
531 efficiency curves on the interpretation of the size of inhaler-generated aerosols. *AAPS*  
532 *PharmSciTech* 14, 497-510.

533 Rowland, M., Cavecchi, A., Thielmann, F., Kulon, J., Shur, J., Price, R., 2018. Measuring the  
534 bipolar charge distributions of fine particle aerosol clouds of commercial PMDI suspensions  
535 using a bipolar Next Generation Impactor (bp-NGI). *Pharm. Res.* 36, 15.

536 Schneider, C.A., Rasband, W.S., Eliceiri, K.W., 2012. NIH Image to ImageJ: 25 years of image  
537 analysis. *Nat. Methods* 9, 671-675.

538 Shah, P.L., Scott, S.F., Geddes, D.M., Conway, S., Watson, A., Nazir, T., Carr, S.B., Wallis,  
539 C., Marriott, C., Hodson, M.E., 1997. An evaluation of two aerosol delivery systems for  
540 rhDNase. *Eur. Respir. J.* 10, 1261-1266.

541 She, P., Wang, Y., Luo, Z., Chen, L., Tan, R., Wang, Y., Wu, Y., 2018. Meloxicam inhibits  
542 biofilm formation and enhances antimicrobial agents efficacy by *Pseudomonas aeruginosa*,  
543 *Microbiologyopen*, 7, e00545.

544 Shekunov, B.Y., Chattopadhyay, P., Tong, H.H.Y., Chow, A.H.L., 2007. Particle size analysis  
545 in pharmaceuticals: principles, methods and applications. *Pharm. Res.* 24, 203-227.

546 Stover, C.K., Pham, X.Q., Erwin, A.L., Mizoguchi, S.D., Warrener, P., Hickey, M.J.,  
547 Brinkman, F.S., Hufnagle, W.O., Kowalik, D.J., Lagrou, M., Garber, R.L., Goltry, L.,  
548 Tolentino, E., Westbrook-Wadman, S., Yuan, Y., Brody, L.L., Coulter, S.N., Folger, K.R., Kas,  
549 A., Larbig, K., Lim, R., Smith, K., Spencer, D., Wong, G.K., Wu, Z., Paulsen, I.T., Reizer, J.,  
550 Saier, M.H., Hancock, R.E., Lory, S., Olson, M.V., 2000. Complete genome sequence of  
551 *Pseudomonas aeruginosa* PAO1, an opportunistic pathogen. *Nature* 406, 959-964.

552 Tay, J.Y.S., Liew, C.V., Heng, P.W.S., 2018. Dissolution of fine particle fraction from  
553 truncated Anderson Cascade Impactor with an enhancer cell. *Int. J. Pharm.* 545, 45-50.

554 Tiddens, H.A., Bos, A.C., Mouton, J.W., Devadason, S., Janssens, H.M., 2014. Inhaled  
555 antibiotics: dry or wet? *Eur. Respir. J.* 44, 1308-1318.

556 van der Wiel, E., Lexmond, A.J., van den Berge, M., Postma, D.S., Hagedoorn, P., Frijlink,  
557 H.W., Farenhorst, M.P., de Boer, A.H., Ten Hacken, N.H.T., 2017. Targeting the small airways  
558 with dry powder adenosine: a challenging concept, *Eur Clin Respir J*, 4, 1369328.

559 Van Schayck, C.P., Donnell, D., 2004. The efficacy and safety of QVAR (hydrofluoroalkane-  
560 beclometasone dipropionate extrafine aerosol) in asthma (Part 2): Clinical experience in  
561 children. *Int. J. Clin. Pract.* 58, 786-794.

562 Vanden Burgt, J.A., Busse, W.W., Martin, R.J., Szeffler, S.J., Donnell, D., 2000. Efficacy and  
563 safety overview of a new inhaled corticosteroid, QVAR (hydrofluoroalkane-beclomethasone  
564 extrafine inhalation aerosol), in asthma. *J. Allergy Clin. Immunol.* 106, 1209-1226.

565 Verbanck, S., Schuermans, D., Paiva, M., Vincken, W., 2006. The functional benefit of anti-  
566 inflammatory aerosols in the lung periphery. *J. Allergy Clin. Immunol.* 118, 340-346.

567 Wang, H., Bhambri, P., Ivey, J., Vehring, R., 2017. Design and pharmaceutical applications of  
568 a low-flow-rate single-nozzle impactor. *Int. J. Pharm.* 533, 14-25.

569 Watts, A.B., Williams, R.O., 2011. Nanoparticles for Pulmonary Delivery, in: Smyth, H.D.C.,  
570 Hickey, A.J. (Eds.), *Controlled Pulmonary Drug Delivery*. Springer, New York, NY, pp. 335-  
571 366.

572 Wimpenny, J., Manz, W., Szewzyk, U., 2000. Heterogeneity in biofilms. *FEMS Microbiol.*  
573 *Rev.* 24, 661-671.

574 Worlitzsch, D., Tarran, R., Ulrich, M., Schwab, U., Cekici, A., Meyer, K.C., Birrer, P., Bellon,  
575 G., Berger, J., Weiss, T., Botzenhart, K., Yankaskas, J.R., Randell, S., Boucher, R.C., Doring,  
576 G., 2002. Effects of reduced mucus oxygen concentration in airway *Pseudomonas* infections  
577 of cystic fibrosis patients. *J. Clin. Invest.* 109, 317-325.

578

579 Table 1. The MICs ( $\mu\text{g/mL}$ ) of tobramycin against *P. aeruginosa* clinical CF isolates and  
580 PAO1 determined in triplicate by macro-dilution method in MH, MMM and ASM media.

581

| <i>P. aeruginosa</i> strain | MICs in MH | MIC in MMM | MICs in ASM |
|-----------------------------|------------|------------|-------------|
| <b>LMG 27649</b>            | 0.5        | 1          | 4           |
| <b>LMG 27643</b>            | 0.5        | 0.25       | 4           |
| <b>LMG 27648</b>            | 1          | 0.5        | 4           |
| <b>PAO1</b>                 | 0.5        | 0.5        | 4           |

582

583

584

585

586

587

588 **Figure legends**

589 **Figure 1.** Schematic of the colony biofilm. Cells were grown on a polycarbonate membrane to  
590 form a biofilm, and on the third day a filter with tobramycin inhalation powder was placed on  
591 top. After incubation for 3 or 24 hours, the cells were harvested and a viable count was  
592 determined.

593 **Figure 2.** The *in vitro* activity of tobramycin against *P. aeruginosa* using the colony biofilm  
594 assay. (A – C) show clinical CF isolates and (D) indicates laboratory strain PAO1. All *P.*  
595 *aeruginosa* biofilms were grown for 48 h on MH agar, treated with 30 µg/disc tobramycin, and  
596 incubated for 24 h at 37°C. The controls represent biofilms without tobramycin. The data  
597 shown represent the standard error of the mean from three biological repeats and each  
598 biological repeat consisted of at least two technical repeats. Statistics were analysed using  
599 unpaired 2-tailed *t* test. Statistically significant differences between treated biofilms (\*\*\*,  
600  $p<0.001$ ; \*\*\*\*,  $p<0.0001$ ) and the control are indicated.

601 **Figure 3.** Aerosol particle size distribution of tobramycin inhalation powder when aerosolised  
602 for 10 seconds from the Podhaler® device into the NGI at 30 L/min (A) and 60 L/min (B).  
603 Error bars represent the standard error of the mean from five independent experiments for each  
604 flow rate. Stages 1-7 indicate the impactor stages, followed by their corresponding cut off  
605 aerodynamic diameter in parentheses. MOC: micro-orifice collector.

606 **Figure 4.** Representative SEM micrographs of TIP particles from NGI stages at different flow  
607 rates. Stage 2, at 30 L/min (A) and Stage 4, at 60 L/min (B). Pictures were taken at x4,000  
608 magnification (scale bar = 5 µm).

609 **Figure 5.** Comparison of the cumulative geometric particle size distributions of tobramycin  
610 inhalation powder particles collected at stage 2 (A) and 4 (B) of the NGI at 30 L/min and 60  
611 L/min, respectively.

612 **Figure 6.** The influence of differently size TIP particles on the eradication of *P. aeruginosa*  
613 biofilms. (A-C) show clinical isolates, and (D) indicates the laboratory strain PAO1. Bacterial  
614 cells were grown as colony biofilms for 48 h at 37°C and then were treated with different  
615 tobramycin particle size fractions of  $d_{ac} < 11.7 \mu\text{m}$  and  $d_{ac} < 2.82 \mu\text{m}$  for 3 h. The data shown  
616 represent the standard error of the mean from three biological repeats and each biological repeat  
617 consisted of at least two technical repeats. Statistics were analysed using an unpaired 2-tailed  
618 *t* test. Statistically significant differences between large and small particles are indicated (\*,  
619  $p < 0.05$ ).

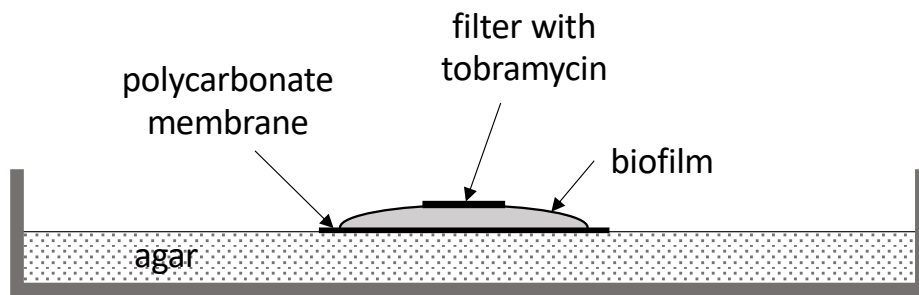
620 **Figure 7.** The influence of differently sized TIP particles on the eradication of *P. aeruginosa*  
621 biofilms. (A-C) show clinical isolates, and (D) indicates the laboratory strain PAO1. Bacterial  
622 cells were grown as colony biofilms for 48 h at 37°C and then were treated with different  
623 tobramycin particle size fractions of  $d_{ac} < 11.7 \mu\text{m}$  and  $d_{ac} < 2.82 \mu\text{m}$  for 24 h. The data shown  
624 represent the standard error of the mean from three biological repeats and each biological repeat  
625 consisted of at least two technical repeats. Statistical significance was analysed using an  
626 unpaired 2-tailed *t* test.

627

628 Figures

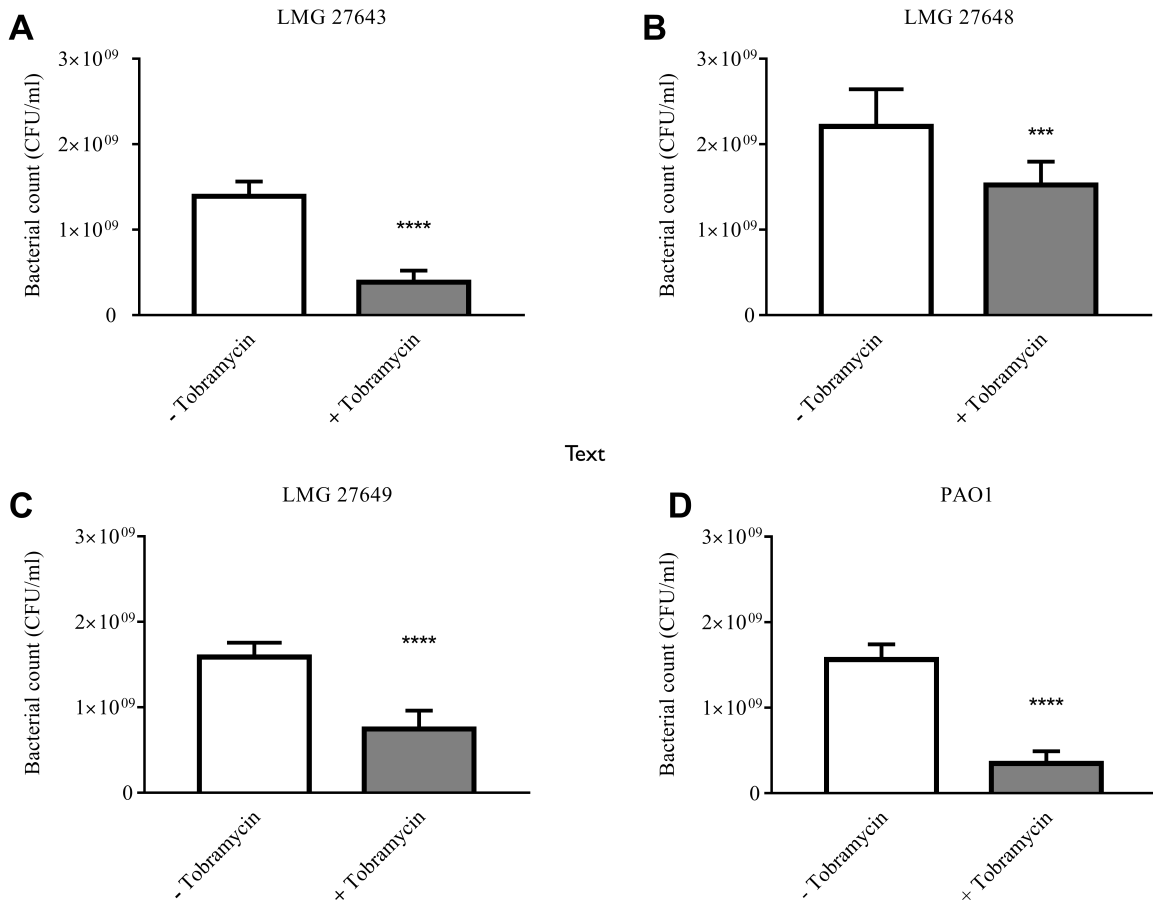
629

630 Figure 1



631

632



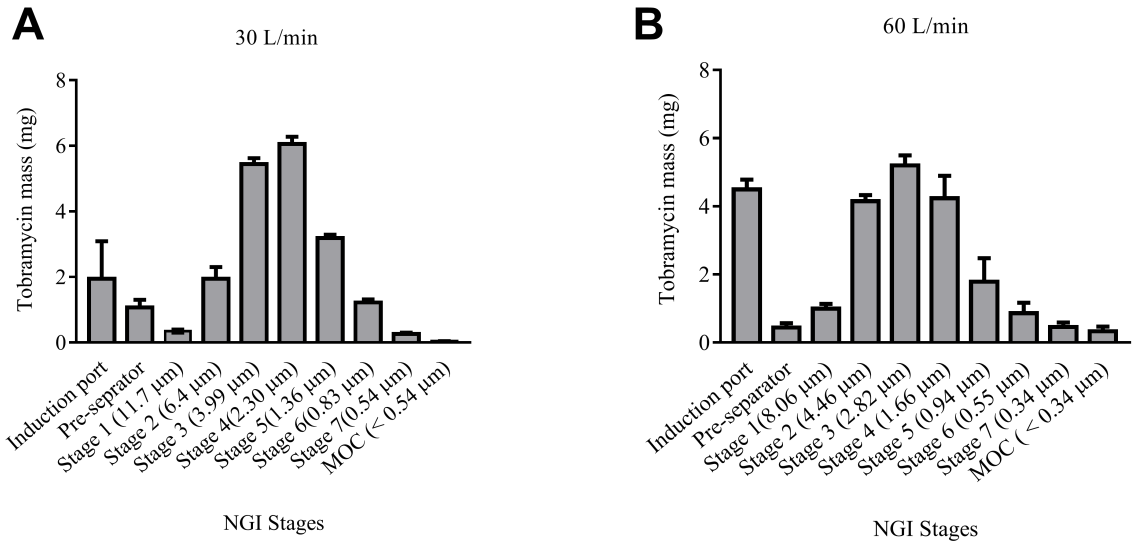
Text

634

635



636 Figure 3



637

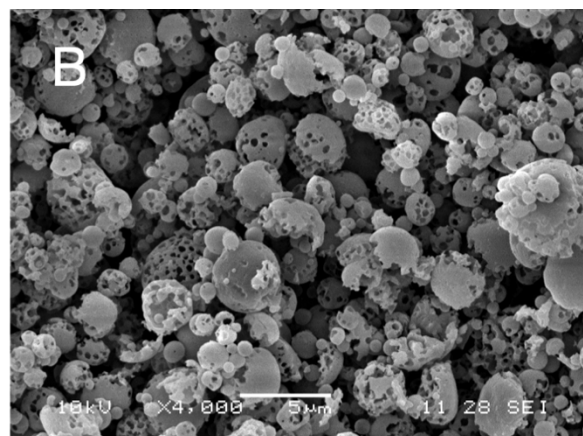
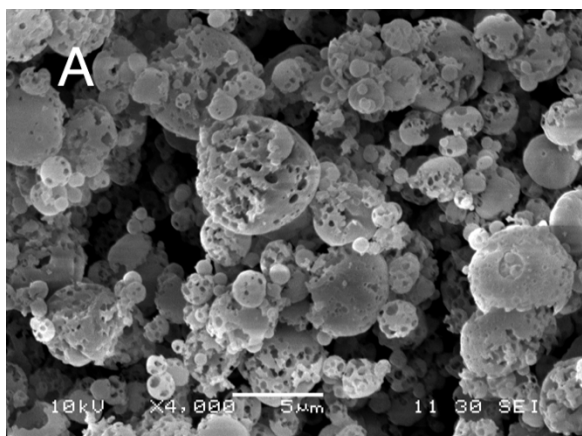
638

639

640

641

642 Figure 4



643

644

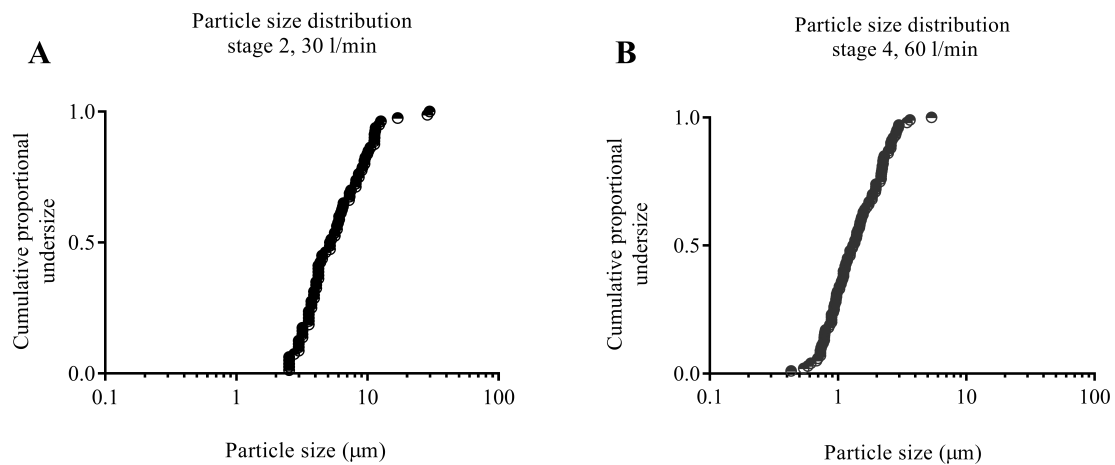
645

646

647

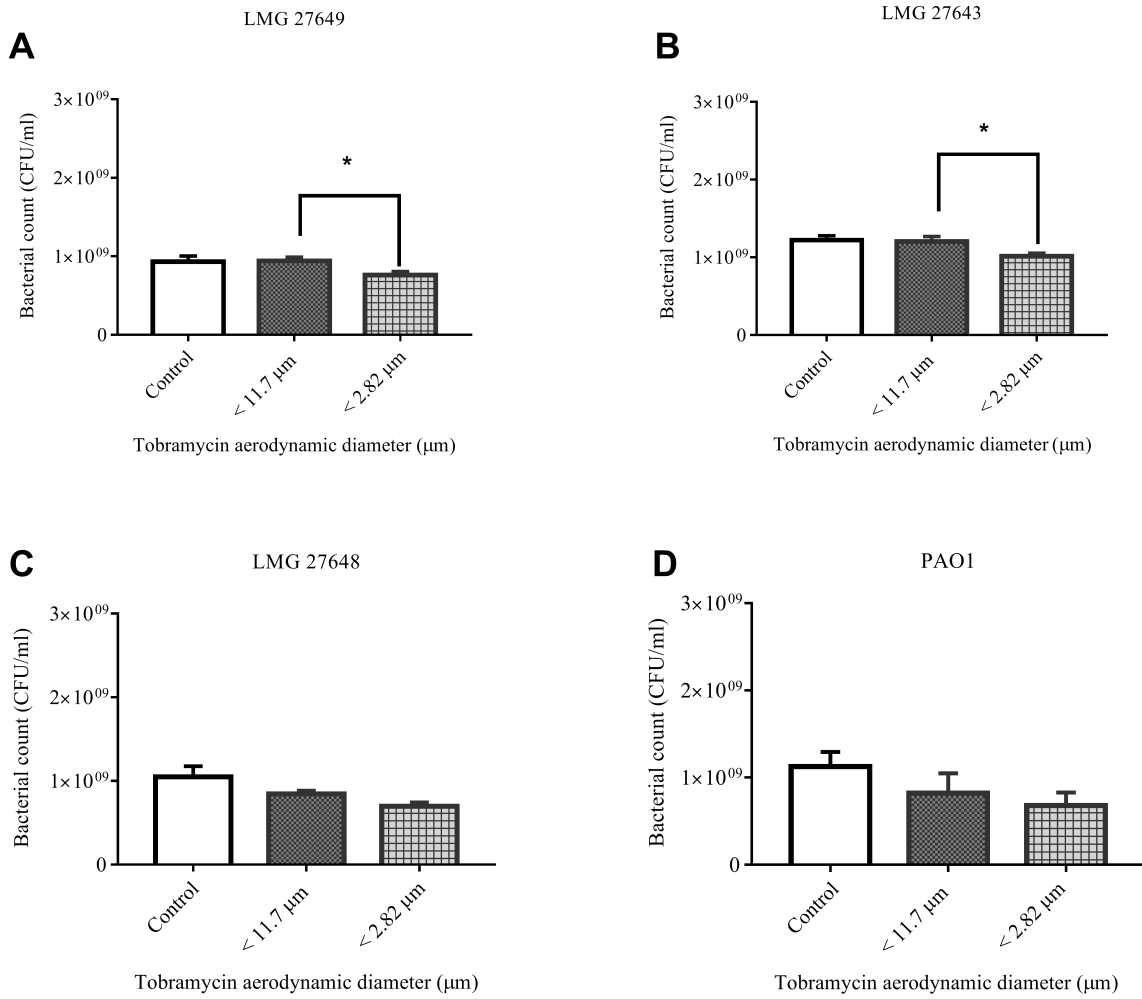
648 Figure 5

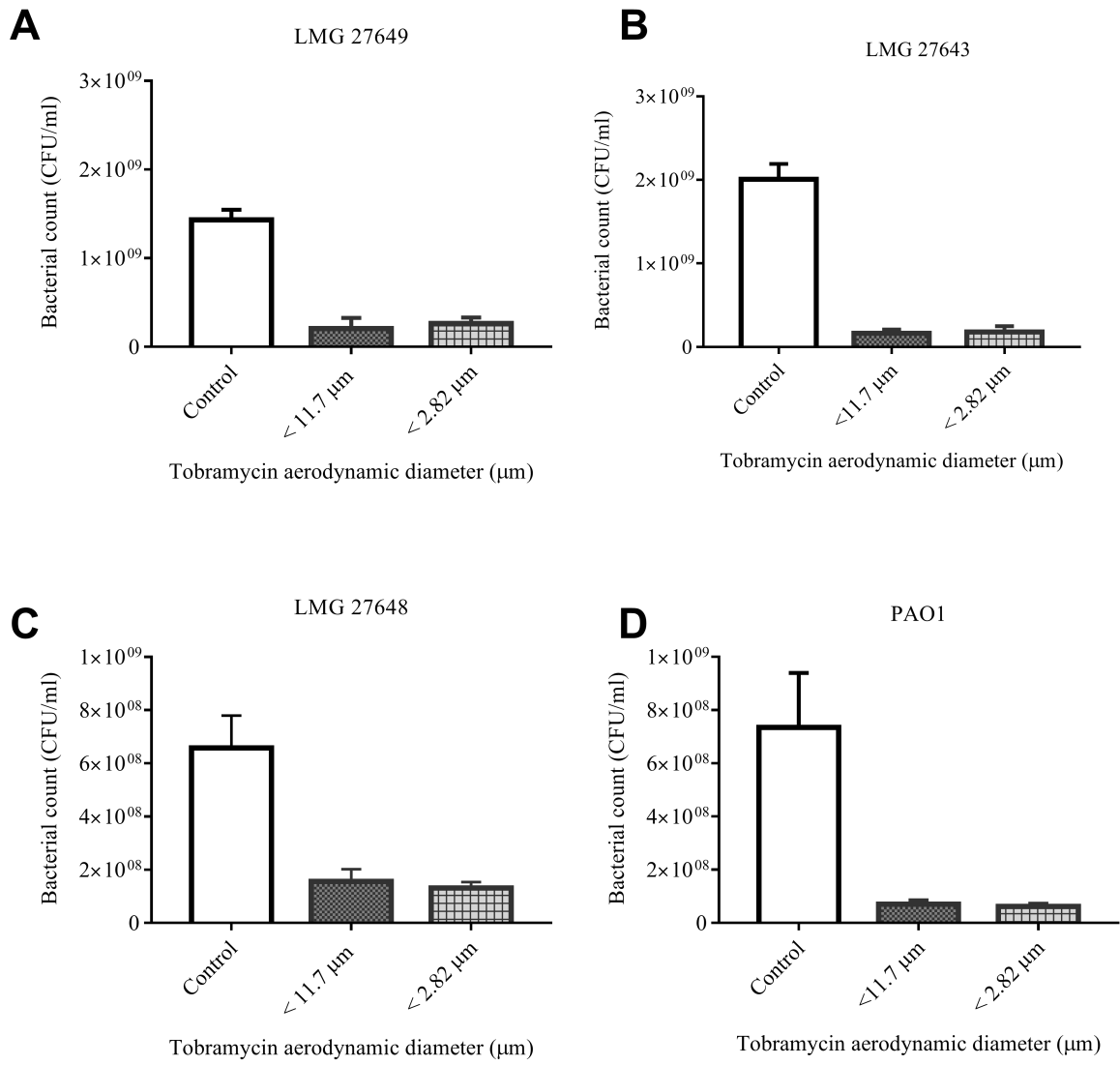
649



650

651





655

656